WiMAX on FSO: Outage Probability Analysis

Nicholas Vaiopoulos, Harilaos G. Sandalidis, and Dimitris Varoutas, *Senior Member, IEEE*

***Abstract*—The transmission of multiple wireless signals over optical links has attained a great research interest nowadays. In case where optical fibers are difficult to be deployed, or installation cost is prohibited, optical wireless systems provide an efficient alternative means. In this paper, we consider the WiMAX (IEEE802.16) standard and construct a simple but adequate scenario to investigate radio signal transmission over terrestrial optical wireless channels. An appropriate system architecture is adopted and a channel model, which entails some of the most critical impairments of the optical channel, i.e., attenuation, turbulence, pointing error effects, as well as of the RF channel, i.e., path loss, shadowing, and Rayleigh fading, is taken into account. The overall link budget and a closed-form of the outage probability of the system are deduced. Several analytical results are depicted using a realistic set of parameter values, to lend a helpful insight to the performance of the proposed architecture.**

***Index Terms*—WiMAX, free space optics (FSO), outage probability, radio on FSO (RoFSO).**

I. Introduction

FREE space optics (FSO) has been recently proposed to reliably transfer multiple wireless signals and this new technology is referred as Radio on FSO (RoFSO). Transmission of radio signals on FSO links combines the benefits for ease of deployment in wireless links and high capacity enabled by fiber optic technologies. Moreover, next generations of FSO systems use seamless connection of free-space beams to optical fibers, eliminating, thus, the necessity to convert transmitted signals from optical to electrical or vice versa [1]. However, the overall performance of outdoor FSO systems depends upon the climatological conditions and the general characteristics of the transmission path. Optical wireless systems are inherently prone to atmospheric attenuation, scintillation, and misalignment effects [2]. All the above factors severely impair the operation of FSO systems as well as the wireless signals being carried by them. Therefore, to attain a high quality of RoFSO networks, proper care is required.

RoFSO technology has also been suggested to provide inexpensive, secure, short-range wireless transport for WiMAX traffic [3]. Worldwide Interoperability for Microwave Access, commonly known as WiMAX, is a telecommunications technology that is based on the IEEE 802.16 standard and is designed to provide affordable wireless broadband services using a variety of transmission modes. In [3], Cvijetic and Wang proposed a terrestrial optical wireless overlay to transmit 802.16-2004 orthogonal frequency-division multiplexing (OFDM) signals through multi-subcarrier modulation, whereas in [4], presented a multi-input multi-output architecture for distributing IEEE 802.16d (WiMAX) traffic. In [5], the authors investigated the transmission performance of the OFDM signals over a turbulent FSO channel. Arnon in [6], suggested a network configuration for WiMAX traffic delivery, including a satellite, several high altitude platforms, and subscribers on the ground, and derived the laser transmitter gain that minimizes the outage probability of the WiMAX link.

A detailed performance analysis of an FSO link carrying WiMAX RF signals is not, however, available in the open technical literature. This is the central motivation of our study. Particularly, we assume a terrestrial laser network configuration and determine the WiMAX quality of service of the laser link model by minimizing the outage probability of the system in total. The overall performance is examined by taking account of a combined channel model which entails some of the most critical impairments of the optical channel, i.e., attenuation, turbulence, pointing error effects, as well as of the RF channel, i.e., path loss, shadowing, and Rayleigh fading.

The rest of the paper is organized as follows. Section II describes the system model under consideration. In section III, the mathematical expressions of the major impairments of the optical sub-channel are given. The path-loss factor is assumed to be deterministic, turbulence follows the log-normal distribution, whereas an efficient distribution for misalignment fading is adopted. The deterministic path-loss, log-normal shadowing, and Rayleigh fading model, considered for the RF sub-channel, are presented in Section IV. In Sections V and VI, novel analytical expressions of the total link budget, considering both the optical and RF sub-channels, and the outage probability are derived, respectively. A set of analytical results is presented in Section VII, whereas some concluding remarks are mentioned in Section VIII.

II. System Model

We consider a terrestrial FSO link which is used to deliver WiMAX traffic from one geographic region to another. The overall system configuration is composed of the optical and the wireless subsystems. The optical subsystem follows, in principle, the one described in [7] and its two basic components include the transmitter and the receiver which are further analyzed below.

Paper approved by W. Shieh, the Editor for Optical Transmission and Switching of the IEEE Communications Society. Manuscript received August 8, 2011; revised February 8, 2012.

N. Vaiopoulos is with the Department of Informatics and Telecommunications, University of Athens, Panepistimiopolis, GR-15784 Athens, Greece (e-mail: nvaio@di.uoa.gr). He also with the Department of Computer Science and Biomedical Informatics, University of Central Greece, Papasiopoulou 2-4, GR-35100 Lamia, Greece.

H. G. Sandalidis is with the Department of Computer Science and Biomedical Informatics, University of Central Greece, Papasiopoulou 2-4, GR-35100 Lamia, Greece (e-mail: sandalidis@ucg.gr).

D. Varoutas is with the Department of Informatics and Telecommunications, University of Athens, Panepistimiopolis, GR-15784 Athens, Greece (e-mail: D.Varoutas@di.uoa.gr).

Digital Object Identifier 10.1109/TCOMM.2012.071212.110182

We assume that the WiMAX traffic from heterogeneous networks reaches the optical transmitter through an access gateway. The transmitter converts the electrical signal to laser. It is composed of a modulator, a laser driver, a light-emitting diode (LED) or laser, and a telescope as a whole. The modulator converts bits of information into signals according to a chosen modulation format. In general, the modulation of the laser or the LED can be performed directly by changing the current with any discrete or a continuous signal (analog modulation). The driver provides the power for the laser and stabilizes its performance. The laser source converts the electrical signal to optical radiation. Finally, the telescope aligns the laser/LED radiation to a collimated beam and directs it to the receiver. The laser propagates through the atmosphere to the receiver assuming a Gaussian beam wave model.

The receiver uses a direct detection scheme and includes a telescope, a filter, a positive–intrinsic–negative (PIN) photodetector, and a trans-impedance amplifier [7]. The telescope is used to collect the radiation from a large area and focuses it onto the detector. The laser can be concentrated by using lenses and mirrors, or any combination of them. A filter helps to remove the background radiation from entering the receiver which generally creates shot noise and saturates the detector. The optical signal from the output of the filter propagates to the detector, which converts it to an RF electrical signal using a PIN photodetector. Finally the trans-impedance amplifier makes the electrical signal stronger. Depending on cost restrictions and reliability requirements, a tracking and pointing subsystem may be implemented in both sides of the communication link to maintain transmitter–receiver alignment [8].

The electrical signal is guided to a WiMAX base station and delivered to the users located there. As already known, the WiMAX standard is based on the OFDM standard utilizing a large number of closely spaced orthogonal subcarriers. In that way, a frequency selective channel is transformed into a number of flat fading subchannels [9]. Each subcarrier is modulated with a conventional modulation format, e.g., M-QAM as considered in the present study. The total electrical power is available for transmission over the number of subcarriers, let say N, in the WiMAX cell area served by the specific base station. Therefore, the received electrical power on a given subcarrier is obtained by dividing the total electrical power by N.

III. FSO Model

The optical channel state, h, is considered to be a product of three factors, i.e. [10],

$$h = h_l h_a h_p, \tag{1}$$

where h_l expresses the path-loss, h_a the atmospheric turbulence, and h_p the geometric spread and pointing errors. We particularly assume that the scintillation has a much smaller correlation time (10-100 msec) as compared with misalignment fading and therefore, these two impairments are considered to be independent [11].

A. Atmospheric loss

The atmospheric loss over a propagation path of length d_o is determined by the exponential Beers-Lambert Law as [10]

$$h_l\left(d_o\right) = \exp\left(-\sigma d_o\right). \tag{2}$$

The attenuation coefficient, σ, results from the superposition of various scattering and absorption processes and is given by

$$\sigma(\lambda) = \frac{3.912}{V}\left(\frac{\lambda_o}{550}\right)^{-\delta}, \tag{3}$$

where

$$\delta = \begin{cases} 1.6, & V > 50km \\ 1.3, & 6km < V < 50km \\ 0.585V^{1/3}, & V < 6km \end{cases}, \tag{4}$$

V is the visibility in km, and λ_o is the transmission wavelength in nm [12].

B. Atmospheric turbulence model

We assume that the intensity fluctuation probability density function (pdf) is modeled as a log-normal distribution. Log-normal pdf is considered to be very effective in weak turbulence conditions and when the receiver's aperture is larger than the correlation length of irradiance fluctuations (e.g., when aperture averaging takes place) [2]. The log-amplitude of the optical intensity has a Gaussian pdf with log-amplitude variance, σ_χ^2, which is related to the Rytov variance as

$$\sigma_\chi^2 \approx \frac{\sigma_R^2}{4}. \tag{5}$$

Moreover, the Rytov variance can be expressed as [2]

$$\sigma_R^2 = 1.23 C_n^2 k^{\frac{7}{6}} d_o^{\frac{11}{6}}, \tag{6}$$

where the refractive-index structure parameter, C_n^2, is considered constant for horizontal paths and $k = 2\pi/\lambda_o$. Based on the above, the intensity pdf is given as [10]

$$f_{h_a}\left(h_a\right) = \frac{1}{2h_a\sqrt{2\pi\sigma_\chi^2}} \exp\left(-\frac{\left(\ln h_a + 2\sigma_\chi^2\right)^2}{8\sigma_\chi^2}\right). \tag{7}$$

C. Pointing Errors

A well-known pointing error model when the distance between the laser transmitter and receiver is not so large was recently launched by Farid and Hranilovic in [10]. By assuming a Gaussian spatial intensity profile of beam waist radius, w_{do}, on the receiver plane, the fraction of the collected power due to geometric spread can be approximated as

$$h_p(a) \approx A_0 \exp\left(-\frac{2a^2}{w_{do_{eq}}^2}\right), \tag{8}$$

where A_0 is the fraction of the collected optical power at $a = 0$ and equals to $\left[\mathrm{erf}\left(\upsilon\right)\right]^2$, a is the radial displacement from the origin of the optical detector, $w_{do_{eq}}^2 = w_{do}^2\sqrt{\pi}\mathrm{erf}(\upsilon)/2\upsilon\exp\left(-\upsilon^2\right)$, $\upsilon = \sqrt{\pi}r/\sqrt{2}w_{do}$, r is the radius of circular aperture of the optical detector, and $\mathrm{erf}(\cdot)$ is the error function [13, eq. 8.250.1]. By considering independent identical Gaussian distributions for the elevation and the horizontal displacement (sway) both of variance σ_s^2, the radial displacement follows a Rayleigh distribution. Then, the pdf of h_p is given by

$$f_{h_p}(h_p) = \frac{\gamma^2}{A_0^{\gamma^2}} h_p^{\gamma^2-1}, \qquad 0 \le h_p \le A_0, \tag{9}$$

where $\gamma = w_{do_{eq}}/2\sigma_s$.

IV. RF Model

The RF model incorporates path loss, log-normal shadowing, and fast Rayleigh fading. The main characteristics of these factors are given in the following subsections.

A. Path loss

To determine the path loss between the base station and the wireless user, we use the following simplified model as a function of distance [14, eq. 2.39]

$$P_{R-RF} = P_{T-RF} K \left(\frac{d_{RFO}}{d_{RF}}\right)^{\nu}, \tag{10}$$

where P_{R-RF} is the received power by the wireless user, P_{T-RF} the transmitted RF power, K a unitless constant which depends on the antenna characteristics and the average channel attenuation, d_{RF} the distance between the RF transmitter and the wireless user, d_{RFO} a reference distance for the antenna far-field, and ν is the RF path loss exponent. When the above model is used to approximate empirical measurements, K is sometimes set to the free space path gain [14, eq. 2.7]. Then, the signal path power attenuation is expressed by

$$P_{R-RF} = P_{T-RF} \left(\frac{\lambda_{RF}\sqrt{G_l}}{4\pi d_{RFO}}\right)^2 \left(\frac{d_{RFO}}{d_{RF}}\right)^{\nu}, \tag{11}$$

where $\sqrt{G_l}$ is the product of the RF transmitted and received antenna field patterns in the line-of-sight direction.

B. Composite Multipath/Shadowing RF Model

In this section, we describe the composite fast fading/shadowing model. Assuming log-normal shadowing, we define ξ to be a log-normally distributed random variable (RV) with variance σ_ξ^2 and pdf

$$f_\xi(\xi) = \frac{10/\ln 10}{\xi\sqrt{2\pi\sigma_\xi^2}} \exp\left(-\frac{(10\log_{10}\xi)^2}{2\sigma_\xi^2}\right), \quad \xi \ge 0. \tag{12}$$

The pdf of Rayleigh fading with variance σ_ψ^2 is expressed as

$$f_\psi(\psi) = \frac{1}{2\sigma_\psi^2} \exp\left(-\frac{\psi}{2\sigma_\psi^2}\right). \qquad \psi \ge 0, \tag{13}$$

Considering that the Rayleigh fading and the log-normal shadowing are independent, the composite pdf of $u = \xi\psi$ can be evaluated using the formula for the density of the product of two independent RVs,

$$f_u(u) = \int f_{u|\xi}(u|\xi) f_\xi(\xi) d\xi, \tag{14}$$

as

$$f_u(u) = \int_0^\infty \frac{10/\ln 10}{2\sigma_\psi^2 \xi^2 \sqrt{2\pi\sigma_\xi^2}} \exp(-\frac{u}{2\sigma_\psi^2 \xi}) \times \exp\left(-\frac{(10\log_{10}\xi)^2}{2\sigma_\xi^2}\right) d\xi. \tag{15}$$

Unfortunately, an analytical expression for (15) does not exist. However, according to [15], a new log-normal distribution can accurately approximate (15) for high values of σ_ξ ($\sigma_\xi \ge 6$ dB), i.e.,

$$f_u(u) \approx \frac{10/\ln 10}{u\sqrt{2\pi\sigma_u^2}} \exp\left(-\frac{(10\log_{10}u - \mu_u)^2}{2\sigma_u^2}\right), \tag{16}$$

where

$$\mu_u = 10\log_{10}(2\sigma_\psi^2) - 2.5dB, \quad \sigma_u = \sqrt{\sigma_\xi^2 + 5.57^2 dB}. \tag{17}$$

Equation (16) can be written in a more concise form as

$$f_u(u) = \frac{1}{u\sqrt{2\pi\sigma_{\ln u}^2}} \exp\left(-\frac{(\ln u - \mu_{\ln u})^2}{2\sigma_{\ln u}^2}\right), \tag{18}$$

where

$$\mu_{\ln u} = (\frac{\ln 10}{10})\mu_u, \quad \sigma_{\ln u} = (\frac{\ln 10}{10})\sigma_u. \tag{19}$$

V. Link budget

For the FSO model under consideration, the received optical power at the WiMAX base station is determined by the well known Friis transmission equation [8]

$$P_{R-O} = P_{T-O} n_T n_R G_{T-O} G_{R-O} \left(\frac{\lambda_o}{4\pi d_o}\right)^2 h, \tag{20}$$

where P_{R-O}, n_R, and G_{R-O} are the optical power, efficiency, and telescope gain of the receiver and P_{T-O}, n_T, G_{T-O} of the transmitter, respectively. The optical power is converted to RF using a square-law device after multiplied by a constant K_{O-RF} as [6]

$$P_{T-RF} = K_{O-RF} (P_{R-O})^2. \tag{21}$$

Equation (21) refers to the total RF transmitted power. Keeping in mind that the number of sub-carriers used is N, the RF transmitted power per subcarrier is obtained as

$$P_{T-RF,sub} = P_{T-RF}/N. \tag{22}$$

By considering the composite RF channel model from the WiMAX base station to the wireless users that includes path loss as described in (11), log-normal shadowing, and fast Rayleigh fading, the overall received power at the wireless terminal is expressed as

$$P_{R-RF,sub} = P_{T-RF,sub} \left(\frac{\lambda_{RF}\sqrt{G_l}}{4\pi d_{RFO}}\right)^2 \left(\frac{d_{RFO}}{d_{RF}}\right)^{\nu} u, \tag{23}$$

where λ_{RF} is the wavelength of the RF signal. Substituting (20) and (21) in (23) and using (1), we have

$$P_{R-RF,sub} = \frac{K_{O-RF}}{N} \times \left(P_{T-O} n_T n_R \left(\frac{\lambda_o}{4\pi d_o}\right)^2 G_{T-O} G_{R-O} h_l \right)^2 \times \left(\frac{\lambda_{RF}\sqrt{G_l}}{4\pi d_{RFO}}\right)^2 \left(\frac{d_{RFO}}{d_{RF}}\right)^\nu h_p^2 h_a^2 u. \quad (24)$$

Since h_a follows a log-normal distribution, the pdf of $H_a = h_a^2$, is derived after a simple transformation of the RV, h_a, as

$$f_{Ha}(H_a) = \frac{1}{4H_a\sqrt{2\pi\sigma_\chi^2}} \exp\left(-\frac{\left(\ln H_a + 4\sigma_\chi^2\right)^2}{32\sigma_\chi^2}\right). \quad (25)$$

Similarly, the pdf of $H_p = h_p^2$, is deduced as

$$f_{H_p}(H_p) = \frac{\gamma^2}{2A_0^{\gamma^2}} H_p^{\frac{\gamma^2-2}{2}}, \qquad 0 \le H_p \le A_0^2. \quad (26)$$

Hence, (24) can be written in a more compact form as a product of a deterministic and a probabilistic factor, namely

$$P_{R-RF,sub} = Aw, \quad (27)$$

where

$$A = \frac{K_{O-RF}}{N}\left(P_{T-O} n_T n_R \left(\frac{\lambda_o}{4\pi d_o}\right)^2 G_{T-O} G_{R-O} h_l \right)^2 \times \left(\frac{\lambda_{RF}\sqrt{G_l}}{4\pi d_{RFO}}\right)^2 \left(\frac{d_{RFO}}{d_{RF}}\right)^\nu, \quad (28)$$

and

$$w = H_p H_a u. \quad (29)$$

The RV w is a product of three independent RVs. To evaluate its pdf, we first define θ as $\theta = H_a u$. We observe that θ is the product of two log-normal RVs and hence according to [16, eq. 11.15], follows a log-normal pdf

$$f_\theta(\theta) = \frac{1}{\theta\sqrt{2\pi(\sigma_{\ln u}^2 + (4\sigma_\chi)^2)}} \times \exp\left(-\frac{\left(\ln\theta - (\mu_{\ln u} - 4\sigma_\chi^2)\right)^2}{2(\sigma_{\ln u}^2 + (4\sigma_\chi)^2)}\right). \quad (30)$$

The above equation can be rewritten as

$$f_\theta(\theta) = \frac{1}{\theta\sqrt{2\pi\zeta^2}} \exp\left(-\frac{(\ln\theta - \lambda)^2}{2\zeta^2}\right), \quad (31)$$

where

$$\lambda = \mu_{\ln u} - 4\sigma_\chi^2, \qquad \zeta = \sqrt{\sigma_{\ln u}^2 + (4\sigma_\chi)^2}. \quad (32)$$

Now, the pdf of $w = \theta H_p$ can be derived using the formula of the product of two RVs, presented in (14), as

$$f_w(w) = \frac{\gamma^2}{A_0^{\gamma^2}} w^{\frac{\gamma^2-2}{2}} \int_{w/A_0^2}^{\infty} \theta^{-\frac{\gamma^2}{2}} \times \frac{1}{2\theta\sqrt{2\pi\zeta^2}} \exp\left(-\frac{(\ln\theta-\lambda)^2}{2\zeta^2}\right) d\theta. \quad (33)$$

The above integral can be easily solved with a proper variable substitution and use of [13, eq. 2.33.1], leading to

$$f_w(w) = \frac{\gamma^2}{4A_0^{\gamma^2}} w^{\frac{\gamma^2-2}{2}} \exp\left(-\frac{\gamma^2(4\lambda - \zeta^2\gamma^2)}{8}\right) \times \mathrm{erfc}\left(\frac{\ln(\frac{w}{A_0^2}) - \lambda + \frac{\zeta^2\gamma^2}{2}}{\zeta\sqrt{2}}\right), \quad (34)$$

where erfc$(\cdot)$ is the complementary error function [13, eq. 8.250.4].

The cumulative distribution function (cdf) of w can be deduced using [17, eq. 06.27.21.0011.01] as

$$F_w(w) = \frac{1}{2}\left[\exp\left(\frac{\gamma^2 f_0(w)}{2} - \frac{\zeta^2\gamma^4}{8}\right)\mathrm{erfc}\left(\frac{f_0(w)}{\zeta\sqrt{2}}\right) + \mathrm{erfc}\left(\frac{\zeta^2\gamma^2/2 - f_0(w)}{\zeta\sqrt{2}}\right)\right], \quad (35)$$

where

$$f_0(w) = \ln(\frac{w}{A_0^2}) - \lambda + \frac{\zeta^2\gamma^2}{2}. \quad (36)$$

VI. Outage Probability

We define the outage probability to be the probability that the received power for a given subcarrier at a given distance, d_{RF}, falls below a minimum received power level target, $P_{\min,sub}$, i.e.,

$$P_{outage,sub} = \Pr(P_{R-RF,sub}(d_{RF}) < P_{\min,sub}), \quad (37)$$

which can also be expressed using (27) by

$$P_{outage,sub} = \Pr(w < \frac{P_{\min,sub}}{A}), \quad (38)$$

or in terms of the cdf of w (see (35)) as

$$P_{outage,sub} = F_w\left(\frac{P_{\min,sub}}{A}\right). \quad (39)$$

Next, we determine the power level target, $P_{\min,sub}$, from the WiMAX standard and the wireless system configuration parameters. For example, we consider that each subcarrier is modulated by the M-QAM modulation scheme[1]. In this vein, we can readily find that the upper-bound of the symbol error rate of the subcarrier is given by [14, eq. 6.25]

$$SER_{sub} \le 4Q\left(\sqrt{\frac{3\overline{SNR_s}}{M-1}}\right), \quad (40)$$

where $Q(\cdot)$ is the Gaussian Q function defined as $Q(x) = 1/\sqrt{2\pi}\int_0^\infty \exp^{-\frac{x^2}{2}} dx$ and also related to the complementary error function erfc$(\cdot)$ by erfc$(x) = 2Q(\sqrt{2}x)$, and $\overline{SNR_s}$ is given by [6]

$$\overline{SNR_s} = \frac{\overline{P_s}T_s}{N_{RF} + N_O}. \quad (41)$$

In the above equation, $\overline{P_s}$ is the average symbol signal power, T_s the symbol duration time, N_{RF} the noise power density due to the front end of the RF subscriber receiver, and N_O

[1]A similar analysis can be conducted by using other modulation formats.

TABLE I
NUMERICAL PARAMETERS

Symbol	Definition	Value
C_n^2	Refractive-index structure parameter	10^{-15} $m^{-\frac{2}{3}}$
d_O	Distance between the optical transmitter and receiver	1 Km
d_{RF}	Distance between the RF transmitter and the wireless user	1 Km
d_{RFO}	RF reference distance	100 m
$\sqrt{G_l}$	Product of the transmit and receive antenna field	44.7 dB
G_{R-O}	Laser receiver telescope gain	112 dB
G_{T-O}	Laser transmitter telescope gain	72 dB
K_{O-RF}	Ratio between the RF power and the square of the optic power	110 dB
M	Constellation size	64
N	Number of sub-carriers in a channel	1024
N_O	Noise power density due to the optical receiver	10^{-22} W/Hz
N_{RF}	Noise power density due to the front end of the RF subscriber receiver	5 10^{-19} W/Hz
n_R	Optics efficiency of the receiver	0.9
n_T	Optics efficiency of the transmitter	0.9
P_{T-O}	Optical transmitted power	40 mW (16 dBm)
SER_{sub}	Symbol error rate	10^{-6}
T_s	Symbol duration time	0.1024 10^{-6} sec
V	Visibility	10 km
λ_O	Laser wavelength	1.55 10^{-6} m
λ_{RF}	Wavelength of RF signal	8.57 10^{-2} m (3.5 GHz)
r	Radius of circular aperture of the optical detector	0.1 m
σ_ξ	Standard deviation of shadowing	8 dB
σ_s	Jitter standard deviation	0.3 m
σ_ψ^2	Variance (Rayleigh fading)	1
ν	RF path loss factor	3.5
w_{do}	Beam radius at 1Km	2 m

the noise power density due to the optical receiver. In most cases, N_O is negligible in comparison with N_{RF} .

Now, we set the minimum power required for acceptable performance for a given subcarrier to be equal to the average symbol signal power, i.e.,

$$P_{\min,sub} = \overline{P_s}. \tag{42}$$

Then, from (40) and (41) we can find the following bound of $P_{\min,sub}$ in terms of SER_{sub}

$$P_{\min,sub} \leq \frac{2(N_{RF}+N_O)(M-1)(\text{erfc}^{-1}\frac{SER_{sub}}{2})^2}{3T_s}. \tag{43}$$

Hence, from (39) the outage probability takes the following form

$$P_{outage,sub} \leq F_w\left(\frac{2(N_{RF}+N_O)(M-1)(\text{erfc}^{-1}\frac{SER_{sub}}{2})^2}{3T_sA}\right). \tag{44}$$

Finally, the outage probability averaged over the N subcarriers can be determined as [5]

$$\mathcal{P}_{outage} = \frac{1}{N}\sum_{n=0}^{N}\mathcal{P}_{outage,sub}. \tag{45}$$

VII. PERFORMANCE EVALUATION

To examine the feasibility of the proposed WiMAX on FSO architecture, we evaluate its performance using a practical set of parameters briefly presented in Table I. These parameters remain constant unless specified below.

At first, we investigate the effect of optical and RF distances on the outage probability. To this end, Fig. 1 visualizes the outage probability in terms of the distance between the RF transmitter and the wireless user for a typical set of laser path lengths, d_o, i.e., from 1 to 5km. A characteristic range of RF distances between 100m and 5km, which represents a conventional area of a WiMAX cell, is taken into account. We can readily observe that for a given optical distance an increase of the RF distance is getting the outage probability worse. Moreover, for a given RF distance the increase of optical length deteriorates the performance. This can be justified as follows. As d_o gets high, both the Rytov variance and the turbulence strength increase (see 5 and 6). Furthermore, the atmospheric loss given by 2 also gets strong. That is, both path loss and turbulence deteriorate, which in turn affect the outage probability.

Secondly, we provide a graph showing the effect of shadowing. Again, the outage probability is plotted in terms of distance d_{RF}. The three curves represent three different standard deviation values of log-normal shadowing, i.e., $\sigma_\xi = 6, 8, 10$ dB. In Fig. 2, we can notice how the performance is affected and we can conclude that the impact of shadowing is quite significant; the greater the shadowing level, the worse the outage probability performance.

To better understand the impact of normalized beamwidth, w_{do}/r, and normalized jitter, σ_s/r, on the outage probability we provide an adequate 3d plot (Fig. 3). It is shown that there is a specific value of w_{do}/r where the outage probability is minimum for a given jitter value. The same also holds if we need to find the optimum jitter for a given beamwidth value. Since proper FSO transmission requires transmitters with accurate control of their beamwidth, a target outage probability can be achieved by selecting an optimum beamwidth which can be obtained using optimization methods, see, e.g., [18].

Finally, in Fig. 4 the impact of constellation size, M, is depicted in terms of the distance between the RF transmitter and the wireless user. It is clear that as the constellation size

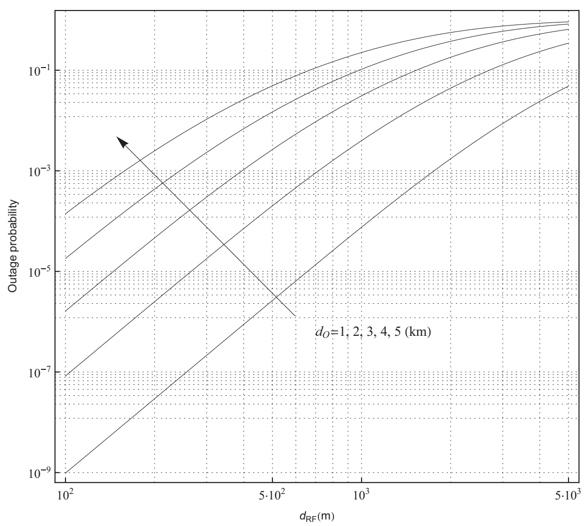

Fig. 1. Outage probability versus distance between the RF transmitter and wireless user for typical optical distances.

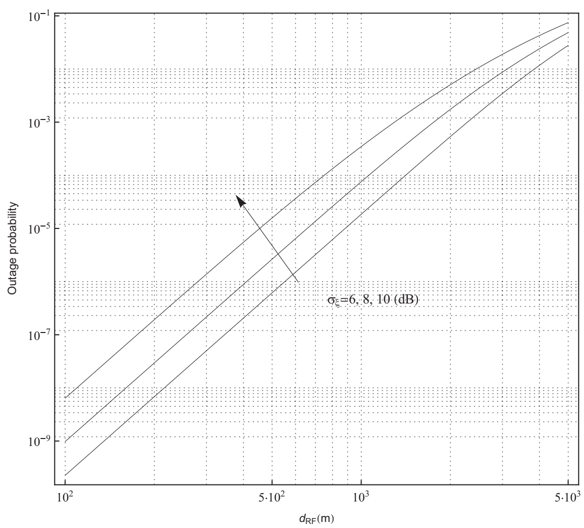

Fig. 2. Outage probability versus distance between the RF transmitter and wireless user for various values of standard deviation of log-normal shadowing.

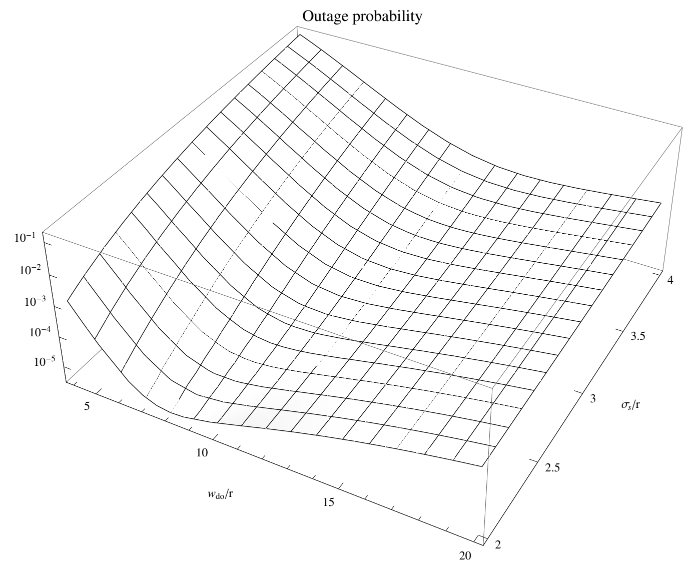

Fig. 3. Outage probability versus normalized beamwidth and jitter.

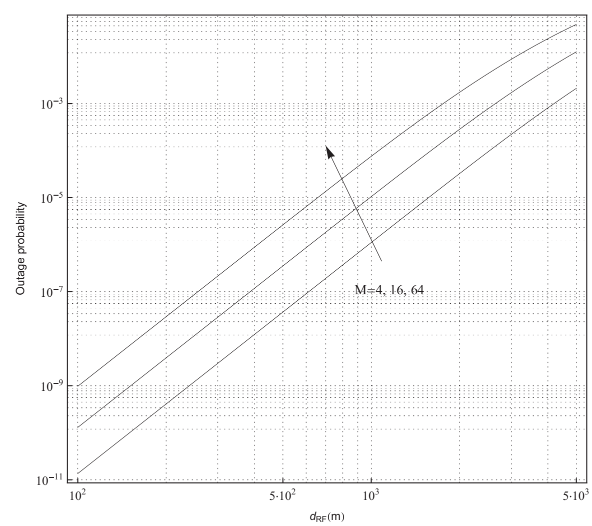

Fig. 4. Outage probability versus distance between the RF transmitter and wireless user for conventional M-QAM constellation sizes.

increases, the requirements in terms of signal power also get high. Keeping in mind that the transmitted power is fixed, it is obvious that the outage probability is getting increased, as well.

VIII. Conclusions

We constructed a simple but adequate architecture to investigate WiMAX transmission over terrestrial FSO channels. The channel model considers the laser link and the WiMAX communication system parameters used in practice. Specifically, some of the most critical impairments of the optical channel, i.e., path loss, turbulence, pointing error effects, as well as of the RF channel, i.e., path loss, shadowing, and Rayleigh fading were taken into account, and an analytical derivation of the outage probability was obtained. The feasibility of the proposed architecture was further evaluated with a realistic set of parameter values and depicted using proper graphs. The present study may constitute the outset of adopting and evaluating more complicated and, at the same time, more realistic RoFSO deployment scenarios. In this vein, the incorporation of forward error correction schemes in order to increase the overall performance seems to be quite challenging and such an extension is a subject of ongoing research carried out by our team.

References

[1] P. T. Dat, A. M. Shah, K. Kazaura, K. Wakamori, T. Suzuki, K. Omae, M. Matsumoto, Y. Aburakawa, K. Takahashi, T. Nakamura, T. Higashino, K. Tsukamoto, and S. Komaki, "Investigation of suitability

of RF signal transmission over FSO links," in *2007 Int. Symp. on High Capacity Opt. Net. and En. Tech*.

[2] L. Andrews and R. L. Philips, *Laser Beam Propagation through Random Media*, 2nd edition. SPIE Press, 2005.

[3] N. Cvijetic and S. G. Wilson, "WiMAX access using optical wireless technology with heterodyne detection in turbulent atmospheric channels," in *Proc. 2006 IEEE GLOBECOM*.

[4] N. Cvijetic and T. Wang, "A MIMO architecture for IEEE 802.16d (WiMAX) heterogeneous wireless access using optical wireless technology," in *Next Generation Teletraffic and Wired/Wireless Advanced Networking*. Springer Verlag, 2006, pp. 441–451.

[5] A. Bekkali, C. B. Naila, K. Kazaura, K. Wakamori, and M. Matsumoto, "Transmission analysis of OFDM-based wireless services over turbulent radio-on-FSO links modeled by gamma-gamma distribution," *IEEE Photon. J.*, vol. 2, no. 3, pp. 510–520, June 2010.

[6] S. Arnon, "Minimization of outage probability of WiMAX link supported by laser link between a high-altitude platform and a satellite," *J. Opt. Soc. Am. A*, vol. 26, no. 7, pp. 1545–1552, July 2009.

[7] ——, "Optical wireless communications," in *Encyclopedia of Optical Engineering*, R. G. Driggers, C. Hoffman, and R. Driggers, editors. CRC Press, 2003, pp. 1866–1886.

[8] ——, "Optimization of urban optical wireless communications systems," *IEEE Trans. Wireless Commun.*, vol. 2, no. 4, pp. 626–629, July 2003.

[9] M. Maqbool, M. Coupechoux, and P. Godlewski, "Comparison of various frequency reuse patterns for WiMAX networks with adaptive beamforming," in *Proc. 2008 IEEE VTC – Spring*.

[10] A. A. Farid and S. Hranilovic, "Outage capacity optimization for free-space optical links with pointing errors," *J. Lightw. Technol.*, vol. 25, pp. 1702–1710, July 2007.

[11] H. G. Sandalidis, T. A. Tsiftsis, and G. K. Karagiannidis, "Optical wireless communication systems with heterodyne detection over turbulence channels with pointing errors," *J. Lightw. Technol.*, vol. 27, no. 20, pp. 4440–4445, Oct. 2009.

[12] H. Willebrand and B. S. Ghuman, *Free Space Optics: Enabling Optical Connectivity in Today's Networks*. Sams Publishing, 2002.

[13] I. S. Gradshteyn and I. M. Ryzhik, *Table of Integrals, Series, and Products*, 7th edition. Academic, 2008.

[14] A. Goldsmith, *Wireless Communications*. Cambridge University Press, 2005.

[15] A. M. Turkmani, "Probability of error for m-branch macroscopic selection diversity," *IEE Proc. -I. Commun. Speech and Vision*, vol. 139, no. 1, pp. 71–78, Feb. 1992.

[16] K. Burry, *Statistical Distributions in Engineering*. Cambridge University Press, 1999.

[17] Wolfram, The Wolfram functions site. Available: http://functions.wolfram.com

[18] H. G. Sandalidis, "Optimization models for misalignment fading mitigation in optical wireless links," *IEEE Commun. Lett.*, vol. 12, no. 5, pp. 395–397, May 2008.